Powder Technology 462 (2025) 121130

Contents lists available at ScienceDirect

Powder Technology

journal homepage: www.journals.elsevier.com/powder-technology

Investigation on ash formation and attrition characteristics of fuel applying to powdered coal-fired circulating fluidized bed boiler system

Manxia Shang [a], Peixing Han [b], Junping Zhu [c], Zhong Huang [a,b,d], Junfu Lyu [a,b,d], Xiwei Ke [b,d,*]

[a] Key Laboratory for Thermal Science and Power Engineering of Ministry of Education, Tsinghua University, Beijing 100084, China
[b] Shanxi Research Institute of Huairou Laboratory, Taiyuan 030006, China
[c] Aiyuan Boiler Group Co., Ltd, Taiyuan 030032, China
[d] Beijing Huairou Laboratory, Beijing 101499, China

HIGHLIGHTS

- A new analysis method on ash formation and attrition characteristics is proposed.
- Primary ash particle size distributions of powdered coal are obtained.
- The attrition rate coefficient of crushed and sieved powdered coal differs greatly.
- Dissimilarity between powdered coals is mainly due to different chemical properties.

GRAPHICAL ABSTRACT

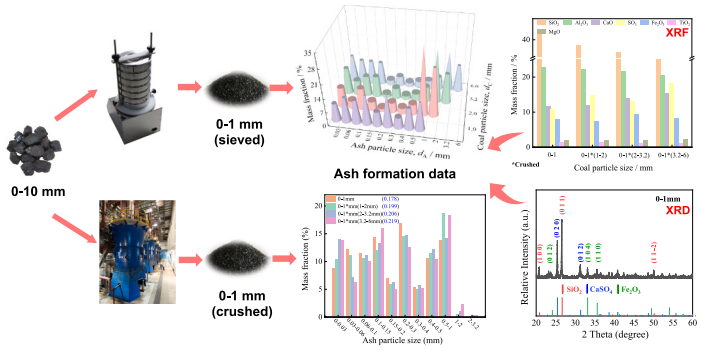

ARTICLE INFO

Keywords:
powdered coal
ash formation
attrition
circulating fluidized bed boiler
material balance

ABSTRACT

Since the mineral distribution of the crushed powdered coal (0-1 mm) differs from that of the sieved powdered coal (0-1 mm), the traditional ash formation characterization method may not apply to the powdered coal-fired circulating fluidized bed (PC-CFB) boiler. Traditional ash formation and powdered coal ash formation experiments were carried out respectively. Results show that the primary ash particle size distribution of the crushed powdered coal is quite different from that of sieved powdered coal. Additionally, the attrition characteristics are related to raw coal size before crushing. The test of physical and chemical properties of ash indicates that the above phenomena can be attributed to the large discrepancy in chemical composition and mineral phases between the two kinds of powdered coal. Finally, the analysis method and data on ash formation and attrition characteristics applicable to PC-CFB boilers are proposed, which facilitate the mathematical modeling of this novel CFB combustion technology.

* Corresponding author at: Shanxi Research Institute of Huairou Laboratory, Taiyuan 030006, China.
E-mail address: kexiwei@sxri.hrl.ac.cn (X. Ke).

https://doi.org/10.1016/j.powtec.2025.121130
Received 18 August 2024; Received in revised form 16 May 2025; Accepted 17 May 2025
Available online 24 May 2025

1. Introduction

The circulating fluidized bed (CFB) has realized the efficient and clean utilization of inferior coal, accounting for about 10% of China's installed capacity of coal-fired plants, and is also the main force to deeply participate in peak regulation of the power grid [1–4]. However, CFB boilers still have the problems of low load regulation rate and high fan energy consumption. To further improve the operational flexibility and reliability of the CFB boiler, Lyu et al. [5,6] proposed the powdered coal-fired circulating fluidized bed (PC-CFB) combustion technology, which combines the advantages of CFB with the excellent combustion characteristics of pulverized coal by reducing the fuel particle size from 0-10 mm to 0-1 mm. In addition to accelerating the combustion rate [7,8], the reduction of fuel particle size affects gas-solid flow parameters such as bed materials' size, circulating flow rate, solid concentration distribution, etc., which influences the heat and mass transfer characteristics inside the furnace, leading to changes in local temperature and atmosphere [9–11]. Thus, this novel CFB combustion technology is expected to improve the combustion efficiency of the boiler, enhance the heat transfer and load regulation capability, and reduce the original emissions of pollutants.

Primary ash particle size distribution (PAPSD), is the particle size distribution of ash particles before entering the steady attrition process [12]. It is known to all that CFB is an "open" system [13], more than 90% of the particles in the circulating system are composed of ash particles. Some research shows that it is complex to maintain material balance if the fuel ash content is too low [14]. The influence of fuel particle size on the above gas-solid flow parameters of the CFB boiler is mainly reflected in the ash distribution and attrition characteristics of the fuel [15,16]. To rationalize the design of the boiler and its auxiliary equipments, it is necessary to understand the ash formation characteristics of coal.

Many experimental studies have been carried out on the ash formation and attrition characteristics of fuel under fluidized bed combustion conditions [17–24]. Previous studies have found that the operating parameters of the boiler have a significant impact on the ash formation and attrition characteristics of fuel. High gas velocities lead to violent particle motion, aggravating the wear between particles and the wall [17,18]. Furthermore, the degree of particle fragmentation and attrition increases with increasing temperature, and the attrition mechanism differs at different temperatures [19,20]. Different grinding equipment can also lead to different ash formation and attrition characteristics [21] of particles.

In addition to the operating parameters, the physical and chemical properties of particles are also the key factors in determining the ash formation and attrition characteristics [17,22–24]. According to the Li et al.'s study, the attrition rate constant (K_{af}) was inversely proportional to the median particle diameter, and it was suggested that the phenomenon was related to the inhomogeneity of the chemical composition distribution [22]. Whereas Tomeczek et al. found that the attrition rate constant was constant for all five particle-size groups for the Silesian sub-bituminous coal [17]. Winter and Liu conducted attrition experiments on three types of coal ash and found that the elements Si and Ca play an important role in ash attrition. The higher the Si content or the lower the Ca content, the less the ash is prone to attrition [23]. Wang et al. investigated the effect of minerals on the K_{af} of four types of coal by using the gray relational analysis (GRA) method. They found that the strength of the effects of the minerals on K_{af} was in the following order: Lime (CaO) > Hematite (Fe_2O_3) >Metakaolinite ($Al_2Si_2O_7$) > Quartz (SiO_2) [24].

For CFB boilers, the raw coal is usually crushed and sieved into coarse particles ranging from 0 to 10 mm. In the traditional ash formation analysis method, the coal particles in the wide sieved range are divided into several continuous size-cut groups and burned separately to obtain the ash particle size distribution (PSD) [22]. While in PC-CFB technology, the raw coal is directly crushed into the powdered coal of 0-1 mm. The following question is whether the ash formation and attrition characteristics of sieved powdered coal obtained in the traditional ash formation analysis method can represent that of the crushed powdered coal in PC-CFB technology. It is well-known that the mineral distribution of most coals is uneven, and large coal blocks usually contain more hard gangue minerals; while the ash core of sieved coal particles is generally smaller and softer in texture, and the ash particle size after combustion is also finer. Therefore, whether the data obtained by the traditional CFB ash formation analysis method can be directly used in PC-CFB boilers remains to be discussed. It is necessary to carry out experiments for further research.

In this paper, three typical types of coal (anthracite, bituminous coal, and lignite) were selected. To explore the differences in the ash formation and attrition characteristics between crushed powdered coal and sieved powdered coal, the traditional ash formation analysis method and powdered coal ash formation analysis method were carried out respectively on each type of coal. In addition, the dissimilarity between crushed powdered coal ash and sieved powdered coal ash in surface morphology, pore structure, and elemental composition was discussed. Based on the above analysis, the analysis method and data on ash formation and attrition characteristics applicable to PC-CFB boiler are proposed, which can provide the input parameters for the mathematical modeling of this novel CFB combustion technology.

2. Experimental section

2.1. Experimental procedure

Some studies have shown that the impacts of coal fragmentation and ash attrition on the final ash particle size distribution are independent under CFB combustion conditions [12,25]. Additionally, the degree of particle attrition is related to the energy provided by the system. Therefore, the ash formation data obtained from mechanical sieving and the results obtained in the fluidized bed system can be converted into each other [26]. On this basis, an experimental test method combining static combustion and cold sieving (SCCS) was developed, in which the pretreated coal is first burnt out in a muffle furnace at a certain temperature [27]. The ash produced is collected and sieved by a sieve shaker with a preset shaking amplitude to simulate the attrition process. This method has been used and described in previous studies [28,29].

To obtain the ash formation and attrition characteristics of 0-1 mm powdered coal, the following experimental scheme was proposed based on the SCCS method [22]: Jiaocheng anthracite (JC), Shuozhou bituminous coal (SZ), and Honghe lignite (HH) were selected in this study. Traditional ash formation and powdered coal ash formation analysis methods were carried out respectively for each type of raw coal. For the traditional ash formation analysis method, the raw coal was sieved into six continuous size-cut groups up to a size of 10 mm (0-1 mm, 1-2 mm, 2-3.2 mm, 3.2-6 mm, 6-8 mm, 8-10 mm), and each group was burned in a muffle furnace at a set temperature of 850°C. The ash was collected and sieved by a sieve shaker with a vertical shaking amplitude of 1.5 mm. In each test, the sieving process lasted at least 100 minutes and was stopped every 10 minutes. During each break, the residual ash in each sieve is weighed. Finally, the ash particle size distributions in each size-cut group were obtained under different attrition times. The attrition process is categorized into a fast attrition process and a steady attrition process. Experimental data showed that it enters a steady attrition process after about 60-min sieving. Combining the PSD data of the feeding coal on the field, the initial ash PSD after the coal is fed into the furnace can be obtained. The attrition rate of ash particles decays with attrition time rapidly and then tends to a constant after a certain period [16]. For a specified particle, the attrition rate R is defined as follows:

$$R = -\frac{1}{m}\frac{dm}{dt}, \ \mathrm{min}^{-1} \tag{1}$$

where m is the mass of particles at a given time and dm/dt is the mass variation rate due to attrition at a certain time interval. The attrition rate

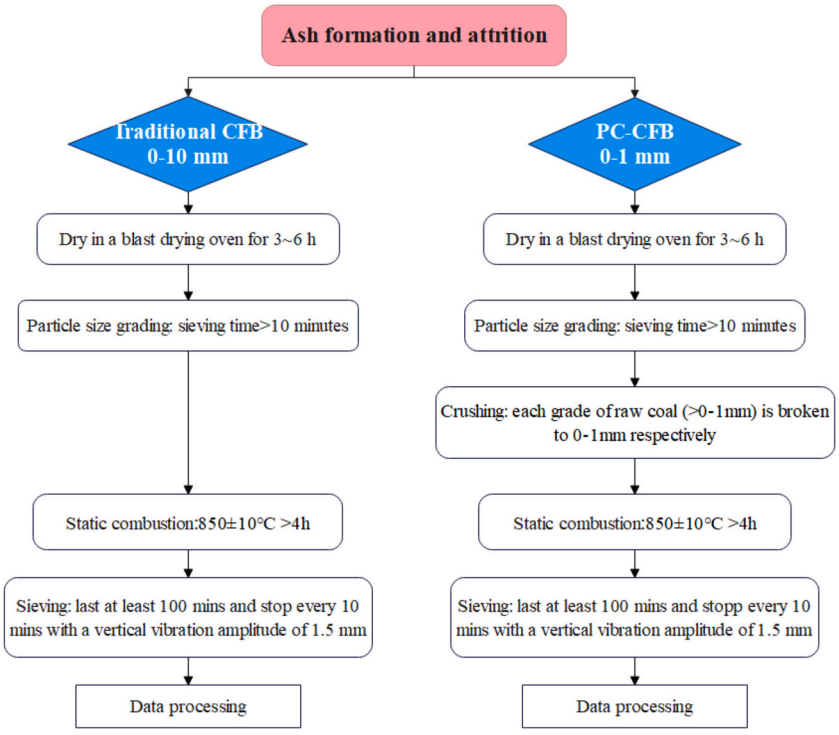

Fig. 1. Flow chart of ash formation and attrition experiments.

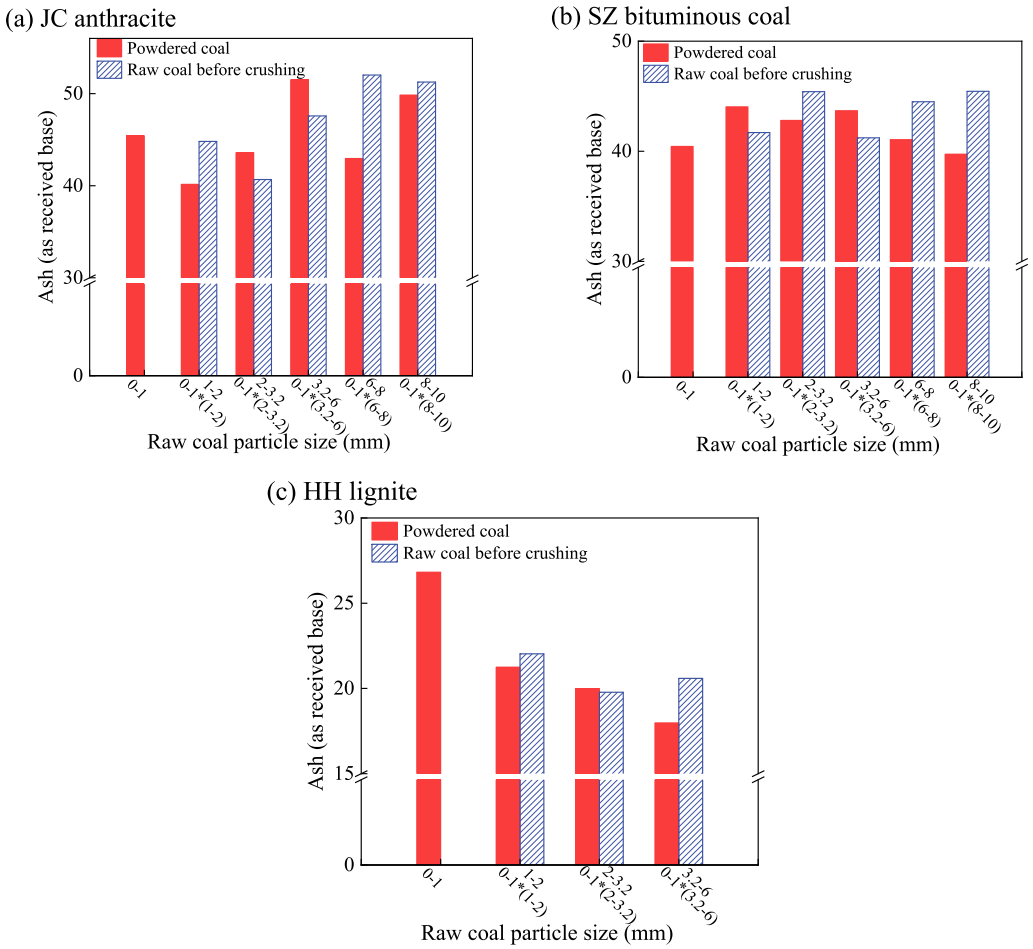

Fig. 2. Ash content of different coals.

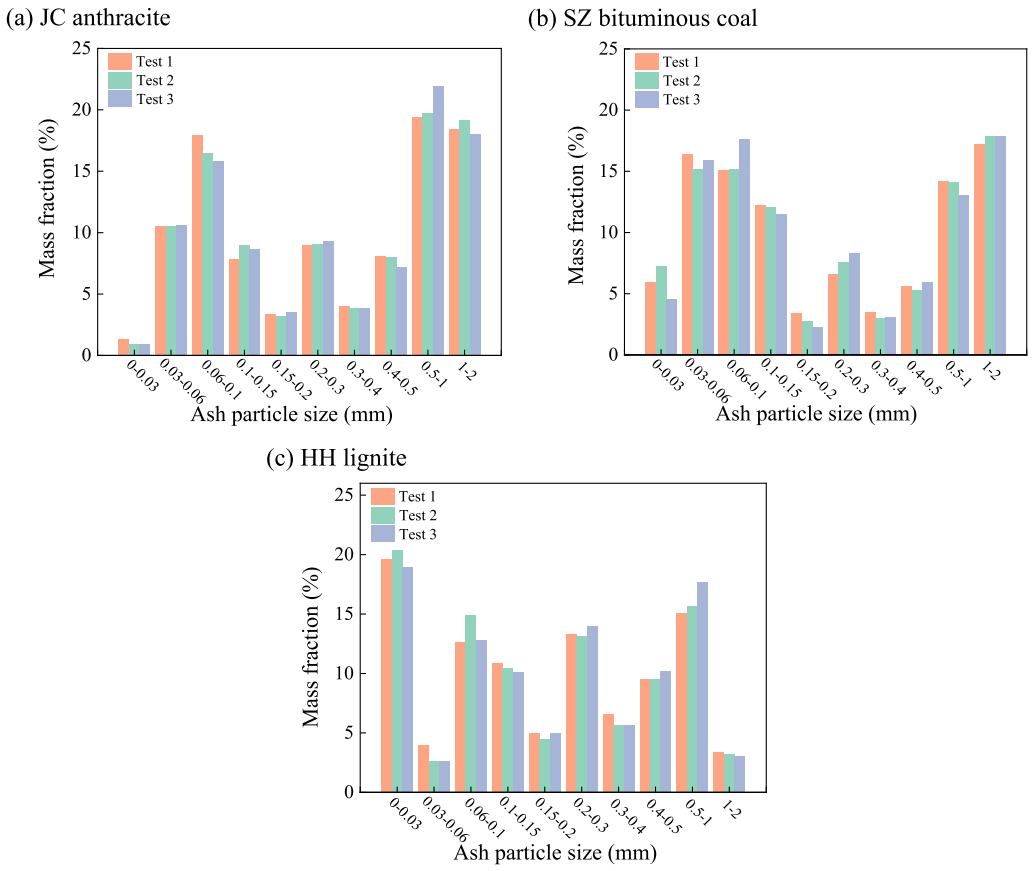

Fig. 3. Results of repetitive experiments for different coals.

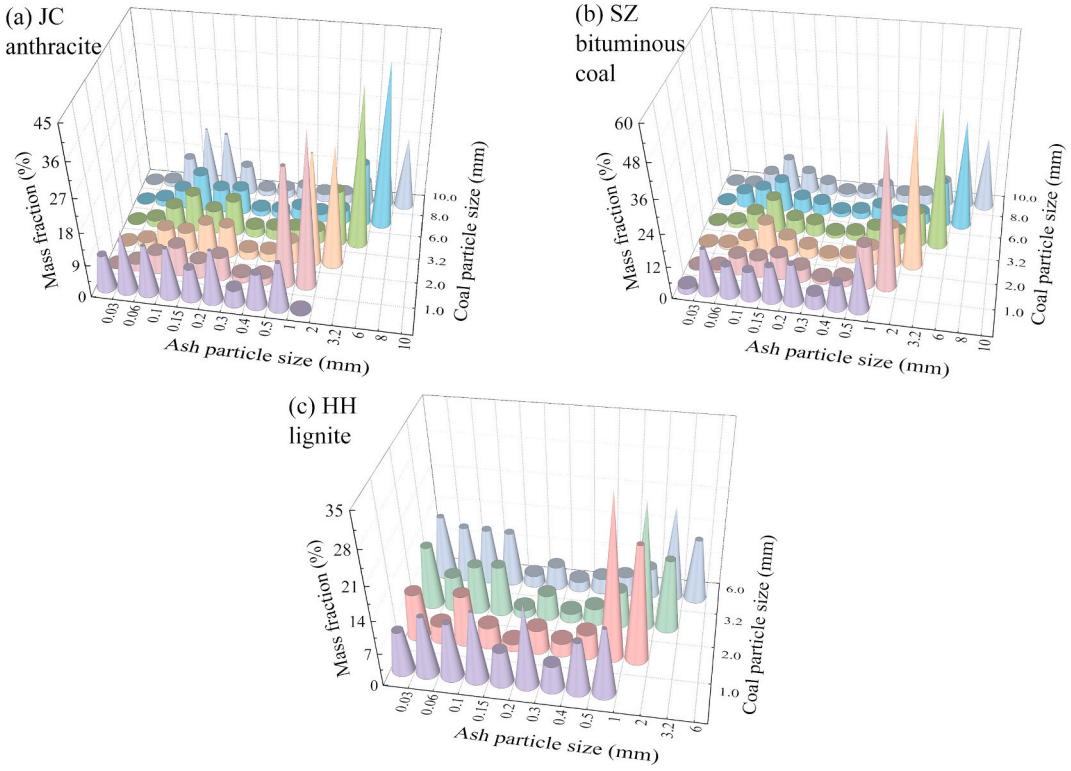

Fig. 4. The PAPSD matrix for different coals.

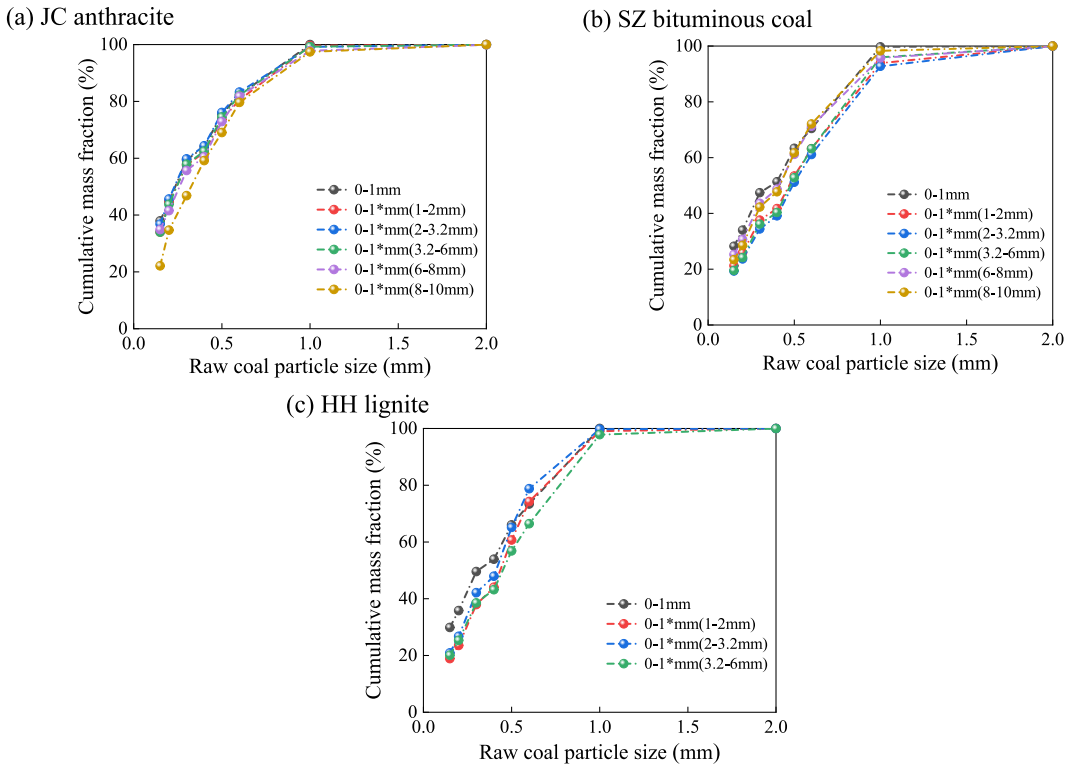

Fig. 5. Particle size distributions of sieved powdered coal and crushed powdered coal.

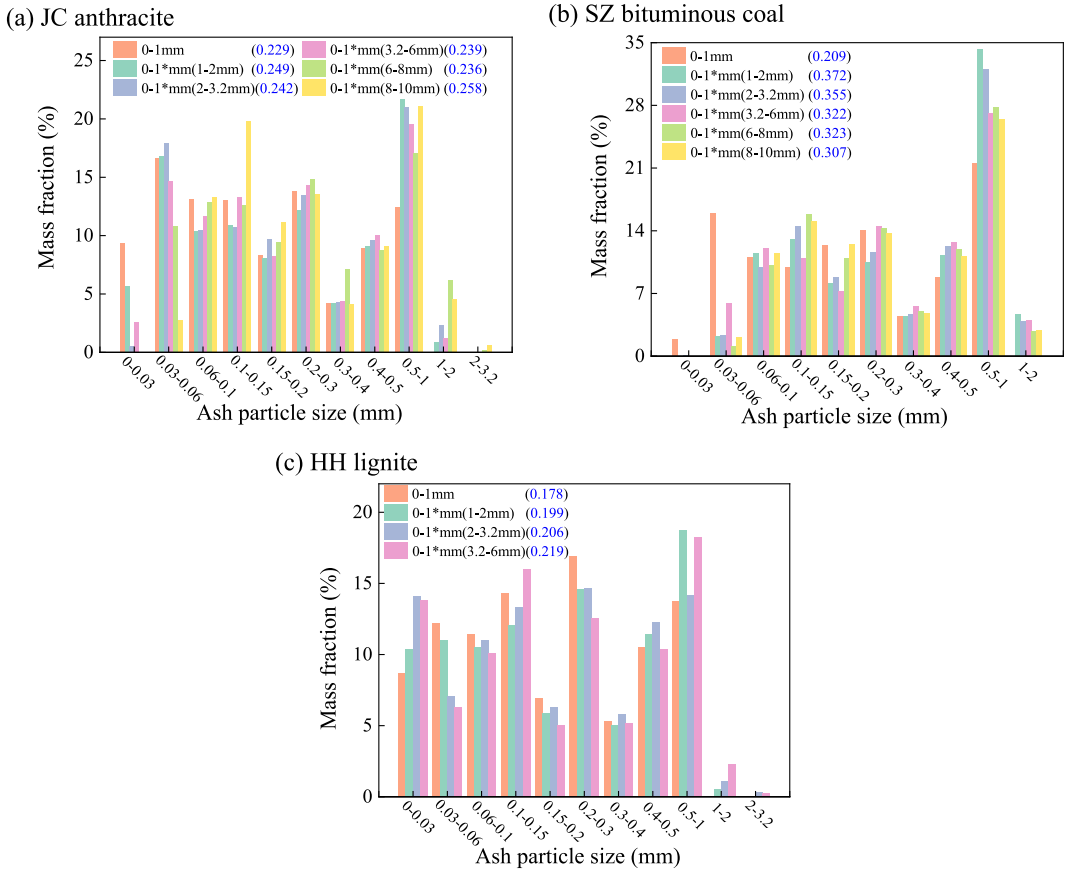

Fig. 6. Powdered coal ash formation data of different coals (the numbers in blue denote median diameter, d_{50}).

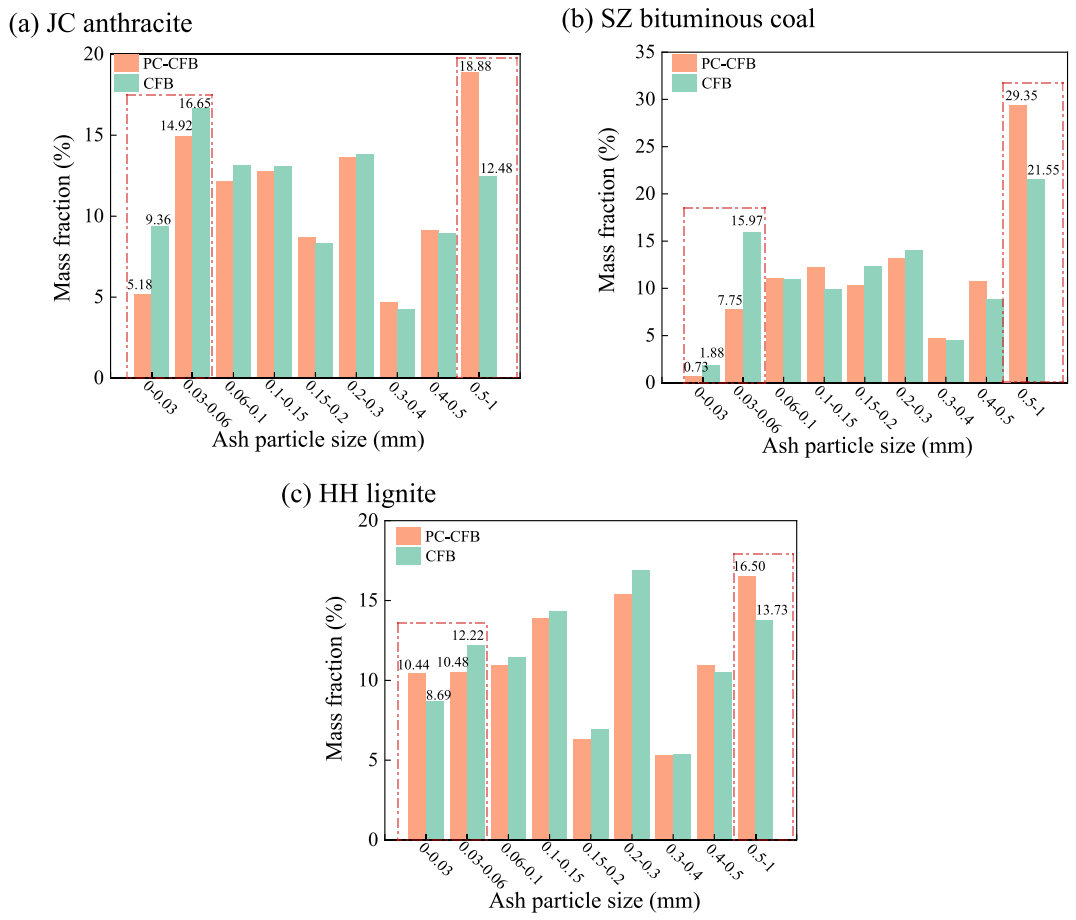

Fig. 7. Comparison of PAPSD of powdered coal obtained by two analysis methods.

coefficient for the cold sieving method is calculated as follows:

$$K_{as} = \frac{R_{as}}{A^2}, \quad m^{-2}\cdot s^{-1} \tag{2}$$

where A is the preset sieving amplitude. For fluidized bed systems, Merrick and Highley developed an attrition model based on Rittinger's criterion, which assumes that the attrition rate of particles in a fluidized bed is proportional to the excess fluidization velocity ($u_g - u_{mf}$) and the attrition rate coefficient [30]. The attrition rate coefficient is defined as:

$$K_{af} = \frac{R_{af}}{u_g - u_{mf}}, \quad m^{-1} \tag{3}$$

where u_g is the surface fluidization velocity, [m·s^{-1}]; u_{mf} is the minimum fluidization velocity, [m·s^{-1}].

For the fluidized bed system, the excitation of the system on the particles can be regarded as the energy provided by the fluidized medium to the solid particles; while in the cold sieving system, the excitation of the system on the particles comes from the energy provided by the mechanical vibration to the solid particles [31]. The effects of these two excitations on the attrition characteristics of ash particles are consistent. According to the energy correlation method, the two attrition rate coefficients have similar decay patterns, and the link between them can be found through standardized data processing:

$$\pi_1 K_{as}(\pi_2 t)A^2 = R'_{as} \Rightarrow R_{af} = K_{af}(u_g - u_{mf}) \tag{4}$$

$$\pi_1 K_{as}(\pi_2 t)A^2 / (u_g - u_{mf}) \Rightarrow K_{af} \tag{5}$$

The attrition rate coefficient K_{af} for the fluidized bed system can be obtained by the transform parameters (π_1 and π_2) between sieving amplitudes and fluidizing velocity [16,27].

For the powdered coal ash formation analysis method, except the 0-1 mm size-cut group, raw coal of other size-cut groups was crushed to 0-1 mm respectively before static combustion, which is called crushed powdered coal (0-1*mm (1-2 mm), i.e., particles of 1-2 mm were crushed to 0-1 mm). The sieved powdered coal and crushed powdered coal are subjected to static combustion and cold sieving in batches to obtain ash formation data. The specific experimental steps are the same as those of the traditional ash formation analysis method, and the experimental procedure is shown in Fig. 1.

2.2. Raw coal properties

Three types of raw coal selected in this work were from Jiaocheng, Shuozhou, and Honghe. The approximate and ultimate analysis was conducted for each size-cut group of raw coal, and detailed data are provided in the Appendix. The ash content of each size-cut group of raw coal is plotted in Fig. 2, which shows that the ash content of the crushed powdered coal from JC anthracite and SZ bituminous coal is generally higher than that of the sieved powdered coal, but HH lignite seems to be an exception. This phenomenon is related to the coal quality, so it is speculated that HH lignite will exhibit different behavior in subsequent ash and attrition tests compared to JC anthracite and SZ bituminous coal.

2.3. Characterization of ash properties

Ash particles (0.4-0.5 mm) from three types of coal were collected to be tested, respectively. JSM-IT800 SEM (Rigaku, Japan) was used to analyze the shape of ash particles. To obtain the elemental composition of the ash, X-ray fluorescence method (XRF) analysis was carried out

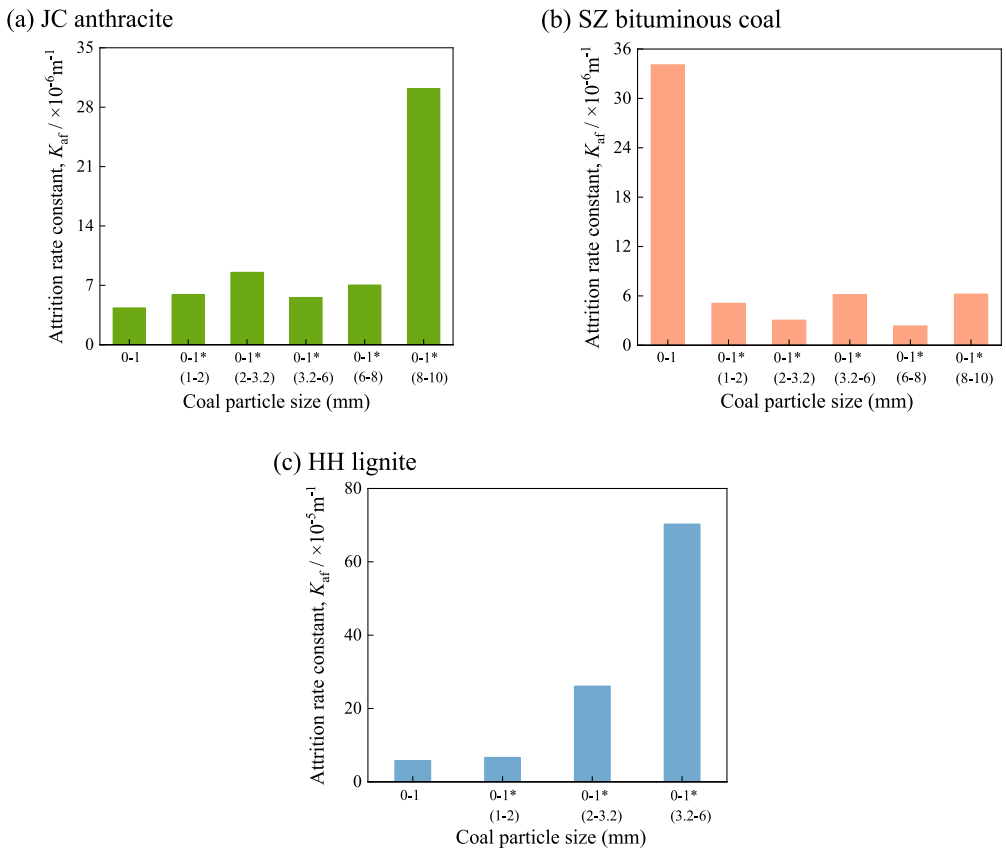

Fig. 8. K_{af} of different coals.

using a ZSX Primus III+ wavelength dispersive XRF analyzer (Rigaku, Japan). Since XRF analysis cannot give the practical existence form of each elemental component in the ash, X-ray diffraction analysis (XRD) was also carried out using a MAXima-X XRD-7000 X-ray diffractometer (Shimadzu, Japan) as a supplement, thus the mineral phases in the ash could be obtained qualitatively.

3. Results and discussion

3.1. Repetitive experiments

To estimate the experimental errors, repetitive experiments were carried out on three kinds of coal respectively, and the primary ash particle size distributions in the tests are shown in Fig. 3. Remarkably, the ash particle size distribution obtained by the repetitive experiments are very similar, and the difference between the maximum and the minimum ash mass fraction is 2.64%. Therefore, it can be asserted that the conclusions drawn within this study are valid.

3.2. Ash formation data

3.2.1. Traditional ash formation analysis method

The PAPSD matrices of JC anthracite, SZ bituminous coal, and HH lignite obtained through traditional ash formation analysis method are shown in Fig. 4. The PAPSD of JC anthracite and SZ bituminous coal are similar, with a high mass proportion of coarse particles (ash particles in the same size-cut group as the raw coal) and a low mass proportion of fine particles (ash particles smaller than 60 μm), and there are two obvious peaks. The PAPSD of HH lignite is different, with a high mass proportion of coarse and fine particles and a low mass proportion of ash particles in the intermediate size-cut group. Compared with JC anthracite and SZ bituminous coal, the difference in PAPSD in each size-cut group of HH lignite is relatively small, with the mass proportion of coarse particles in the ash being lower than 35%.

The attrition process consists of fragmentation and abrasion. The parent particles will produce some daughter particles with relatively small sizes due to the fragmentation of particles, while the abrasion process produces a large number of fine particles much smaller than the parent particles [32]. Therefore, it can be inferred that the primary fragmentation of each size-cut group of HH lignite is deep, and the mass proportion of fine particles produced is relatively high, accounting for about 20%. The reason for this difference is mainly related to the coal quality. Lignite has a low degree of coalification, small hardness, and less ability to resist external mechanical action compared with JC anthracite and SZ bituminous coal, so it is more prone to fragmentation and abrasion in the combustion and attrition process, thus generating more fine particles.

3.2.2. Powdered coal ash formation analysis method

Fig. 5 and Fig. 6 show the PSDs of sieved powdered coal and crushed powdered coal, respectively, and their respective PAPSDs. Although the particle size distributions of raw coal are similar for JC anthracite and SZ bituminous coal, there is still a big difference in PAPSD between crushed powdered coal and sieved powdered coal, and fine particles account for a higher proportion in the sieved powdered coal ash. At the same time, the median particle diameter (d_{50}) of the crushed powdered coal ash is generally higher than that of the sieved powdered coal ash (see legend). For HH lignite, the PAPSD of crushed powdered coal is similar to that of sieved powdered coal, and the mass proportion of fine particles in the crushed powdered coal ash is higher than 20% in all cases.

To compare the PAPSD of powdered coal obtained by the two analysis methods, taking the PSD data of the feeding coal in a power plant as an example, the PAPSD of powdered coal was calculated for three types of raw coal according to the traditional ash formation and

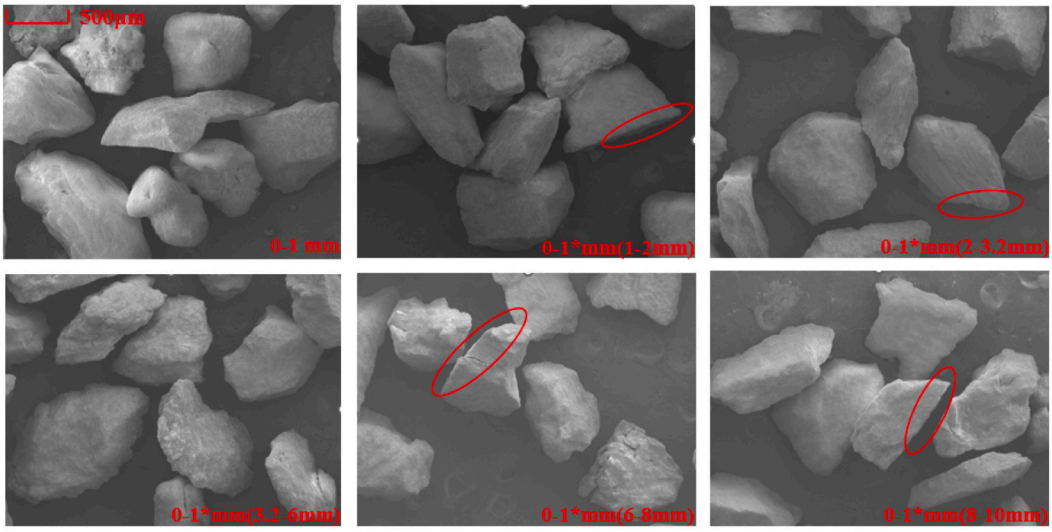

(a) SEM images of JC powdered coal ash

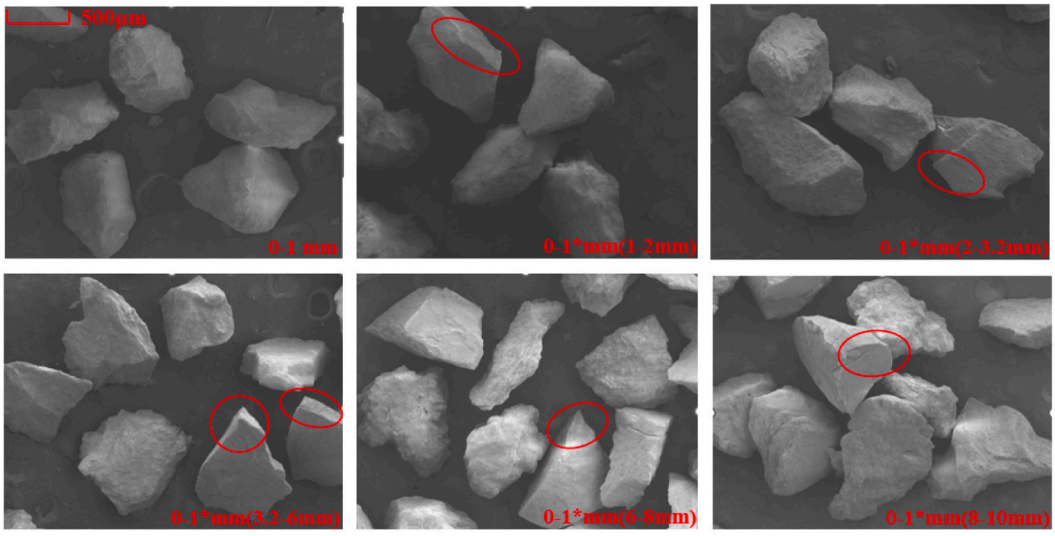

(b) SEM images of SZ powdered coal ash

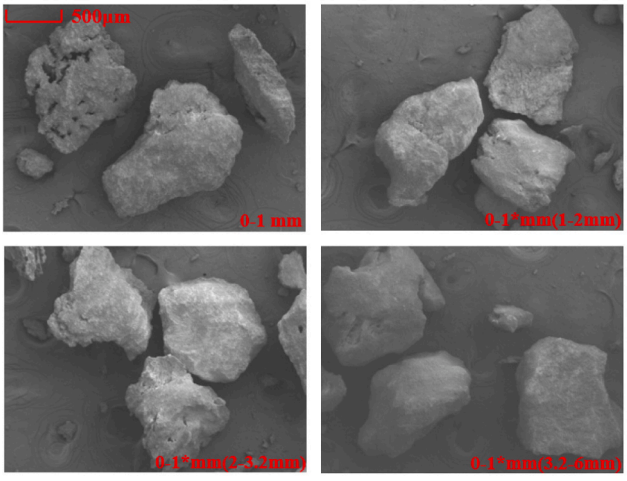

(c) SEM images of HH powdered coal ash

Fig. 9. SEM images of powdered coal ash from different coals.

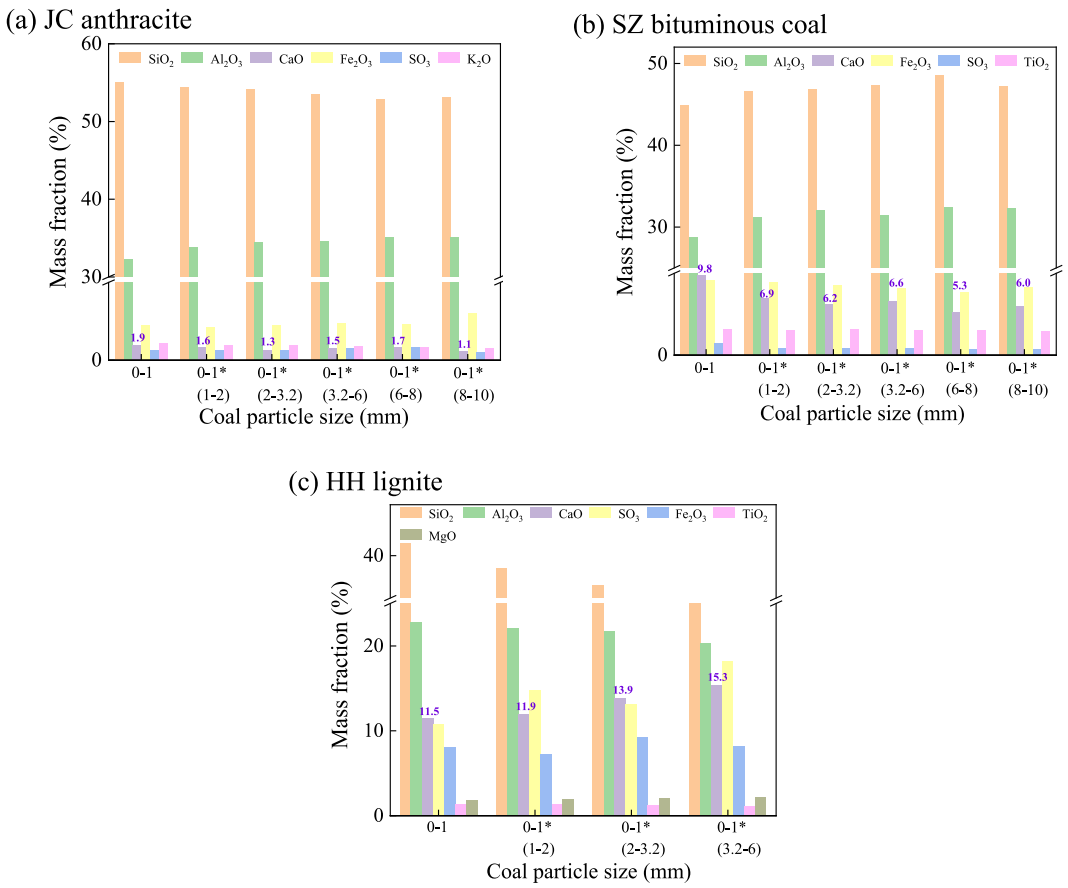

Fig. 10. Elemental contents of powdered coal ash from different coals.

powdered coal ash formation experimental data, respectively, and the results are shown in Fig. 7. It is obvious that the PAPSD of powdered coal obtained by these two methods is close to the same in the range of 0.2-0.5 mm, while the mass proportion at both ends of the distribution differs greatly, especially for JC anthracite and SZ bituminous coal, with a difference of nearly 10%. This could be due to the fragmentation and attrition mechanism. Therefore, the original CFB ash formation data cannot be directly used as the input parameters for PC-CFB boiler calculation.

3.3. Ash attrition characteristics

The attrition rate coefficient K_{af} of the powdered coal obtained by the energy correlation method is shown in Fig. 8. The attrition rate coefficient of HH lignite is significantly higher than that of the other two types of raw coal, indicating that the ash particles formed by this coal are more easily to be rounded and smaller in the boiler. The K_{af} of the three types of coal shows different variation trends among different size-cut groups of powdered coal. The K_{af} of crushed powdered coal from JC anthracite and HH lignite is significantly higher than that of sieved powdered coal, and it tends to increase with the increase of the initial particle size of raw coal. Nevertheless, the K_{af} of powdered coal ash from SZ bituminous coal shows an opposite variation trend with the particle size of raw coal.

It has been suggested that the surface abrasion depends on the total exposed area of ash particles to a certain extent [31]. However, in this investigation, the total exposed area of each size-cut group of powdered coal ash is similar (0.4-0.5 mm), and this factor is not critical in the mode of fragmentation. With this in mind, it's hypothesized that the difference is mainly due to the physical and chemical properties of the ash itself. The analysis and discussion are presented below in conjunction with the test results.

3.4. Physical and chemical properties of ash samples

3.4.1. Surface morphology

The surface morphology of ash particles from the sieved powdered coal and crushed powdered coal was analyzed. Fig. 9 illustrates the surface images of the ash. As can be seen from the SEM images, the shape of ash particles from the sieved powdered coal is generally more regular than that from the crushed powdered coal, and the surface is smoother, while the ash particles from the crushed powdered coal usually have sharp edges with many shape corners. From this point of view, it can be preliminarily inferred that the different surface morphology of the two kinds of ash particles leads to their different performance during the attrition process.

3.4.2. XRF results

The powdered coal ash from the three types of raw coal was subjected to an XRF test. Fig. 10 demonstrates the elemental contents of ash particles obtained by XRF analysis. The major elements of ash particles from the three types of raw coal are Si, Al, Fe, Ca, and S, and the total content of Si and Al is higher than 50%.

Interestingly, the content of each element shows an approximate monotonic variation with the initial particle size of raw coal. For SZ bituminous coal, the larger the initial particle size of raw coal, the higher the Si and Al content, and the lower the Ca and Fe content. Some studies have already shown that high Si and Al content usually correspond to low K_{af}, which makes the ash less prone to attrition [23,24]. High Ca content generally represents soft ash particles, thus the K_{af} of sieved powdered coal from SZ bituminous coal is higher than that of crushed powdered coal.

However, for JC anthracite, the larger the initial particle size of raw coal, the lower the Si content and the higher the Al content. Since the Si

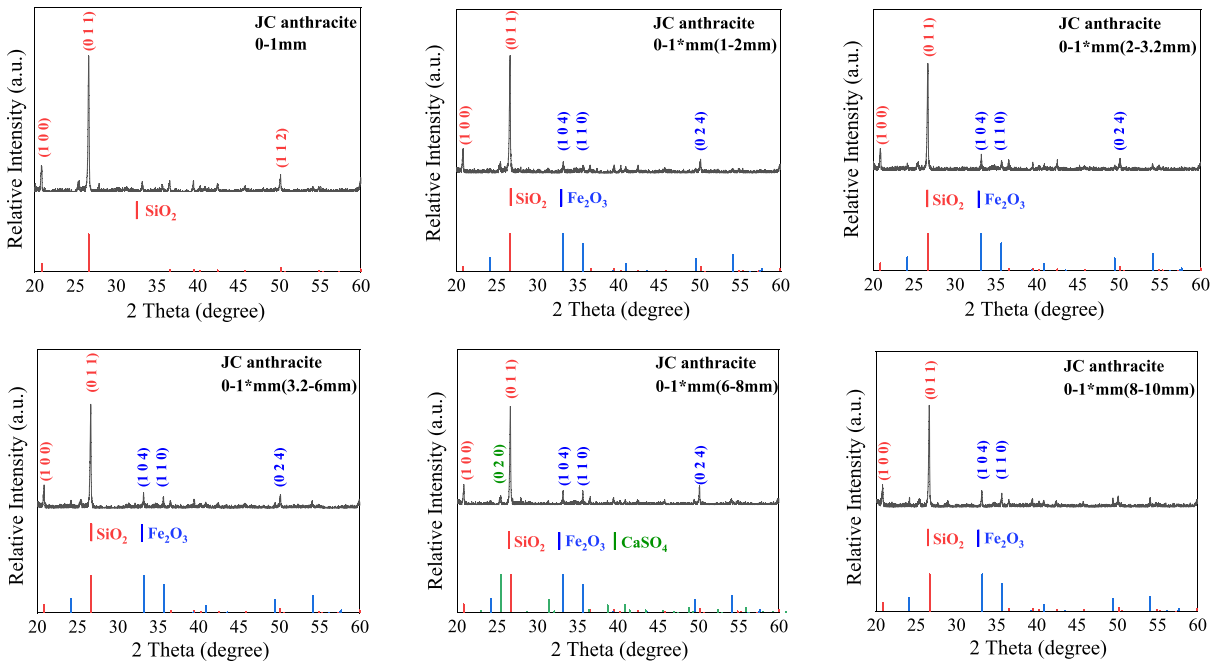

(a) XRD results of JC powdered coal ash

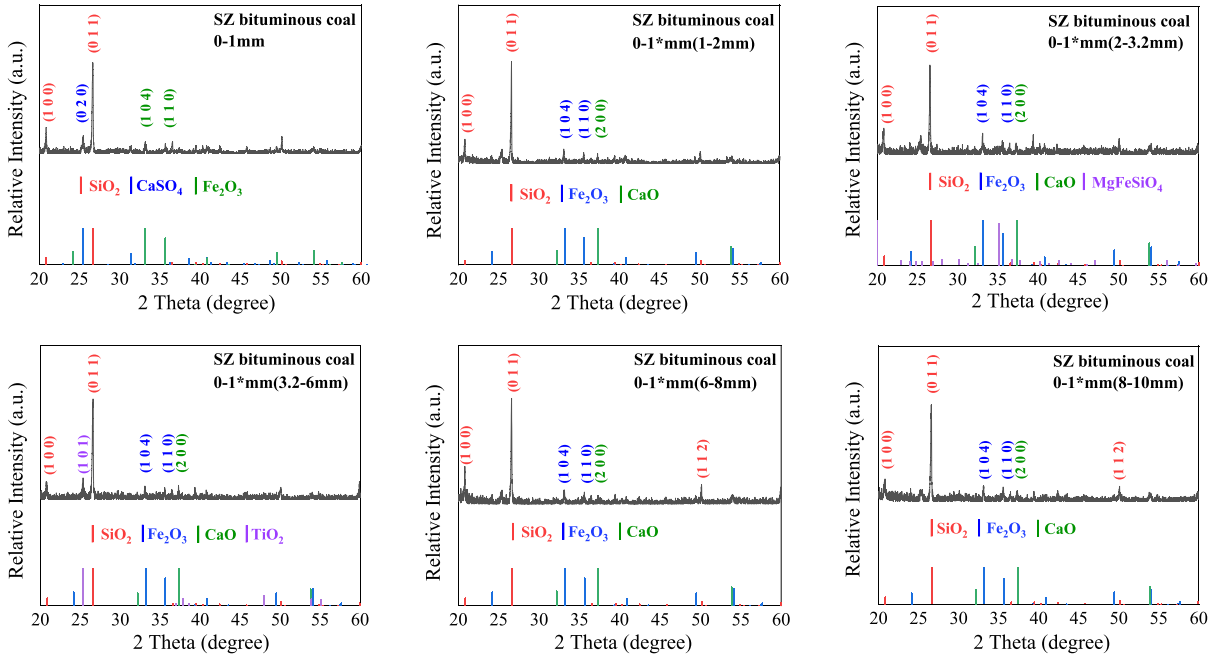

(b) XRD results of SZ powdered coal ash

Fig. 11. XRD results of powdered coal ash from different coals

content is higher than 50%, it can be preliminarily considered that the high Si content leads to the low K_{af} of the sieved powdered coal from JC anthracite.

Distinguishing from JC anthracite and SZ bituminous coal, the ash of HH lignite has a higher content of Ca and S, and the S content of the ash from the 0-1*mm (3.2-6 mm) powdered coal is up to 20%. The crushed powdered coal has lower Si and Al content but higher Ca and S content, thus its K_{af} is higher than that of sieved powdered coal.

XRF analysis can only give results of elemental composition, and the actual existence form of chemical components in ash is the mineral phase. There is a strong need to acquire detailed information on mineral phases in ash, so as to evaluate the effect of minerals on the attrition characteristics of ash effectively and feasibly.

3.4.3. XRD results

The XRD results of ash particles are presented in Fig. 11. It can be observed that SiO_2 and Fe_2O_3 are the major phases in the ash from the three types of raw coal. Although mineral phases such as Fe_2O_3, CaO,

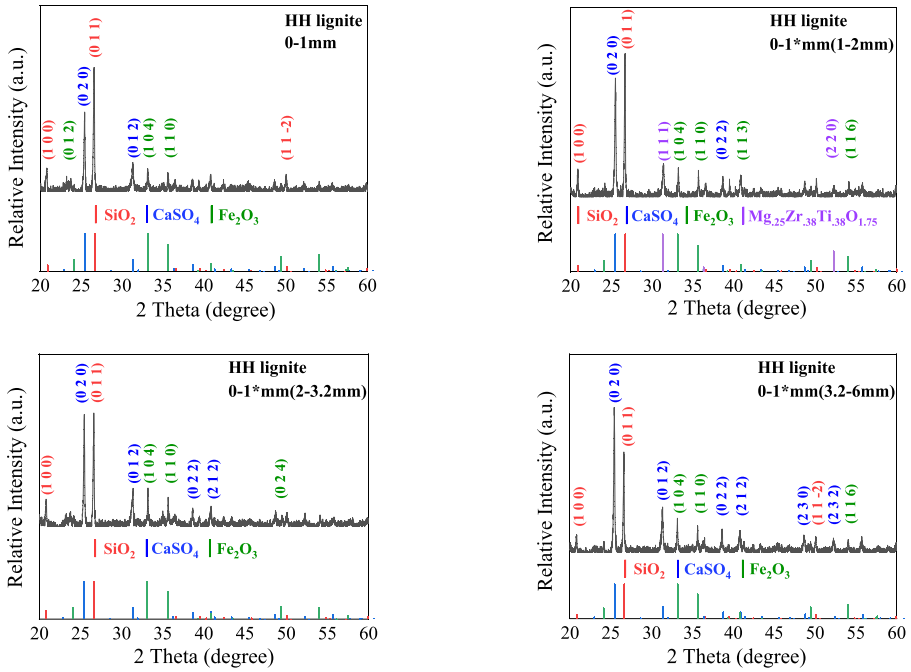

(c) XRD results of HH powdered coal ash

Fig. 11. (*continued*).

Table 1
Pore structure parameters of ash with different particle sizes.

Sample	Size (mm)	Surface area (m^2/g)	a_1 (%)	a_2 (%)	a_3 (%)
JC anthracite	0-1 mm	6.0796	0.5251	47.06	52.41
	0-1*mm(1-2 mm)	5.1617	0.4039	53.75	45.84
	0-1*mm(2-3.2 mm)	6.6261	0.3148	43.42	56.27
	0-1*mm(3.2-6 mm)	5.1868	0.1810	39.63	60.19
	0-1*mm(6-8 mm)	6.5276	0.5108	56.20	43.29
	0-1*mm(8-10 mm)	8.7434	0.4561	55.77	43.77
SZ bituminous coal	0-1 mm	4.8968	0.2858	46.34	53.37
	0-1*mm(1-2 mm)	7.4015	0.3394	61.94	37.72
	0-1*mm(2-3.2 mm)	9.9823	0.7580	61.99	37.25
	0-1*mm(3.2-6 mm)	8.2492	0.4593	62.38	37.16
	0-1*mm(6-8 mm)	8.4236	0.6098	44.95	54.44
	0-1*mm(8-10 mm)	8.1359	0.5377	51.27	48.19
HH lignite	0-1 mm	4.2198	0.1591	32.12	67.72
	0-1*mm(1-2 mm)	16.5869	0.2906	45.21	54.50
	0-1*mm(2-3.2 mm)	5.0019	0.1829	36.42	63.40
	0-1*mm(3.2-6 mm)	11.1984	0.2692	45.85	53.88

a_1-microporous ratio (< 2 nm); a_2-mesoporous ratio (2-50 nm); a_3-macroporous ratio (50-250 nm).

and $CaSO_4$ were detected in the ash from JC anthracite and SZ bituminous coal, the characteristic peaks were not obvious.

In terms of HH lignite ash, the characteristic peaks of $CaSO_4$ and Fe_2O_3 were clearly observed, and the peaks of $CaSO_4$ and Fe_2O_3 gradually enhanced with the increase of the initial particle size of raw coal. Meanwhile, the main peak of $CaSO_4$ is higher than that of SiO_2 in the 0-1*mm (3.2-6 mm) powdered coal, which becomes the major phase in the ash. This phenomenon is in line with the results of XRF analysis. The mineral hardness (on the Mohs Scale) of $CaSO_4$ and Fe_2O_3 is 3.5 and 6, respectively, which is lower than that of SiO_2 (7). Hence, the increase in mass proportion of these soft minerals leads to the elevation of K_{af} of HH lignite ash, i.e., the HH lignite ash is more susceptible to abrasion [24].

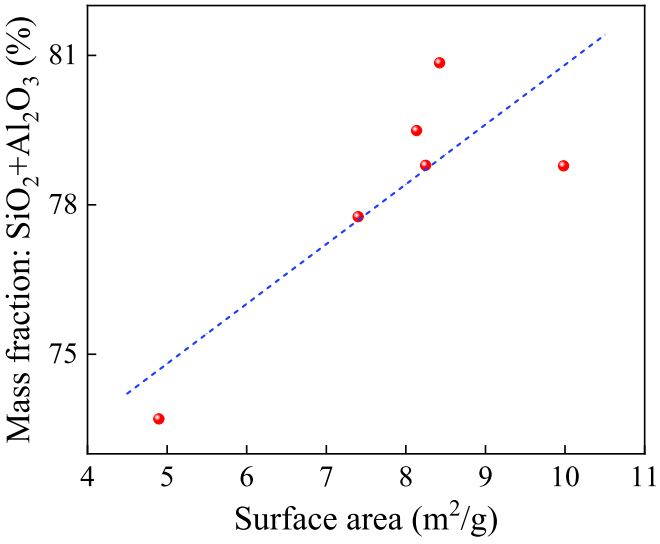

Fig. 12. Variation of surface area with Si and Al content (SZ bituminous coal ash).

3.4.4. *Pore structure analysis*

Additionally, the pore structure of the ash was tested in this study.

The information on the specific surface area and pore distribution (calculated according to BJH adsorption pore distribution data) of the ash particles is listed in Table 1. In general, as the initial particle size of raw coal increases, the specific surface area and the mesoporous ratio of the ash particles increase, and the macroporous ratio decreases. There are obvious differences in the pore structure of ash particles from different powdered coals. The pore structure of ash particles is mainly affected by the distribution of minerals. As shown in Fig. 12, there is a positive correlation between the surface area and the mass fraction of Si and Al. Si and Al mainly exist in the form of aluminosilicate minerals in ash, which have a complex pore structure and a more developed microporous structure. Therefore, the increase in the mass fraction of these substances leads to an increase in the microporous ratio and surface area in the ash. Meanwhile, the content of Ca and S in HH lignite ash is high, and they mainly exist in the form of sulfate, which also has a complex pore structure, and the pore structure of the ash will also be affected.

It proposes an important message that even if the particle size of sieved powdered coal is similar to that of crushed powdered coal, there are still great differences in physical properties such as pore structure. Therefore, for boilers burning fuels prepared by the crushing system, it is not recommended to use the traditional ash formation analysis method to obtain the ash formation and attrition characteristics of the fuel but to refer to the analysis method proposed in this study, where the fuels are grouped and crushed before the combustion and attrition steps are carried out.

4. Conclusions

Based on the static coal combustion and cold ash sieving experiments, traditional and powdered coal ash formation analysis methods were carried out respectively on three types of raw coal (JC anthracite, SZ bituminous coal, and HH lignite). The primary ash particle size distributions (PAPSDs) of sieved and crushed powdered coal with the same particle size were obtained, as well as the ash attrition characteristics. In addition, the surface morphology, and physical and chemical properties of ash particles were analyzed. The conclusions of this study are drawn as follows:

- The PAPSDs of sieved and crushed powdered coal are nearly the same in the range of 0.2-0.5 mm, while the mass proportion at both ends of the distribution differs greatly, especially for JC anthracite and SZ bituminous coal, with a difference of nearly 10%. In addition, the K_{af} of crushed powdered coal from JC anthracite and HH lignite is higher than that of sieved powdered coal, and the K_{af} increases with the initial particle size of raw coal. However, for SZ bituminous coal, K_{af} shows an opposite trend with raw coal particle size. Consequently, the original CFB ash formation and attrition data cannot be directly used for PC-CFB boiler calculation.
- The distributions of chemical composition and mineral phases in sieved and crushed powdered coal differ significantly. The crushed powdered coal from SZ bituminous coal has higher Si and Al content but lower Ca content, which results in lower K_{af}. However, the crushed powdered coal from JC anthracite and HH lignite has lower Si content and more soft minerals such as $CaSO_4$ and Fe_2O_3, resulting in higher K_{af}. Thus, it can be concluded that the difference in physical and chemical properties leads to the significant dissimilarity in ash formation and attrition characteristics between sieved and crushed powdered coal.
- The experimental method and data on ash formation and attrition characteristics applicable to PC-CFB combustion technology are proposed, which can provide significant input parameters for the mathematical modeling of this novel CFB combustion technology.

CRediT authorship contribution statement

Manxia Shang: Writing – original draft, Methodology, Investigation. **Peixing Han:** Methodology. **Junping Zhu:** Project administration. **Zhong Huang:** Writing – review & editing. **Junfu Lyu:** Supervision. **Xiwei Ke:** Supervision.

Declaration of competing interest

The authors declare that they have no known competing financial interests or personal relationships that could have appeared to influence the work reported in this paper.

Acknowledgment

This research was supported by the Key Project of the National Fourteen-Five Year Research Program of China (2022YFB4100303) and the Major Science and Technology Project of Huairou Laboratory.

Appendix A. Approximate and ultimate analysis (as received base) of JC anthracite, SZ bituminous coal, and HH lignite

(a) Jiaocheng coal

Sample	Proximate analysis/%				Ultimate analysis/%				$Q_{net,ar}$/MJ·kg^{-1}
	M_{ar}	A_{ar}	V_{ar}	FC_{ar}	C_{ar}	H_{ar}	N_{ar}	S_{ar}	
0-1 mm	0.37	45.43	10.63	43.57	45.21	2.33	0.67	1.74	16.86
1-2 mm	0.46	44.81	10.32	44.41	45.71	2.58	0.63	2.07	17.00
2-3.2 mm	0.43	40.67	10.32	48.58	49.63	2.48	0.69	2.07	18.74
3.2-6 mm	0.43	47.58	10.33	41.66	42.21	2.22	0.65	2.50	15.70
6-8 mm	0.43	52.02	10.32	37.23	38.12	2.12	0.77	1.22	13.68
8-10 mm	0.57	51.26	10.88	37.29	38.79	2.15	0.64	0.98	14.04
0-1*mm (1-2 mm)	0.39	40.16	10.25	49.2	49.70	2.54	0.72	1.95	18.76
0-1*mm (2-3.2 mm)	0.43	43.58	10.17	45.82	46.76	2.43	0.65	2.10	17.45
0-1*mm (3.2-6 mm)	0.49	51.51	10.04	37.96	38.76	2.10	0.58	1.86	14.06
0-1*mm (6-8 mm)	0.52	42.96	11.06	45.46	47.28	2.49	0.67	1.84	17.70
0-1*mm (8-10 mm)	0.55	49.85	10.41	39.19	41.04	2.26	0.71	1.20	14.97

(b) Shuozhou coal

Sample	Proximate analysis/%				Ultimate analysis/%				$Q_{net,ar}$/MJ·kg^{-1}
	M_{ar}	A_{ar}	V_{ar}	FC_{ar}	C_{ar}	H_{ar}	N_{ar}	S_{ar}	

(continued on next page)

(*continued*)

(b) Shuozhou coal

Sample	Proximate analysis/%				Ultimate analysis/%				$Q_{net,ar}$/MJ·kg^{-1}
	M_{ar}	A_{ar}	V_{ar}	FC_{ar}	C_{ar}	H_{ar}	N_{ar}	S_{ar}	
0-1 mm	0.66	40.44	24.09	34.81	44.12	3.09	0.78	1.11	16.81
1-2 mm	0.84	41.70	24.20	33.26	43.15	3.25	0.74	1.04	16.45
2-3.2 mm	0.94	45.42	22.93	30.71	39.41	3.09	0.68	1.06	14.91
3.2-6 mm	1.22	41.22	23.38	34.18	43.14	3.24	0.75	1.12	16.41
6-8 mm	1.09	44.50	23.86	30.55	40.61	3.17	0.71	0.94	15.32
8-10 mm	1.12	45.45	22.79	30.64	39.42	3.14	0.67	0.99	14.93
0-1*mm (1-2 mm)	0.82	44.04	23.55	31.59	40.62	3.04	0.71	1.00	15.39
0-1*mm (2-3.2 mm)	0.99	42.80	24.06	32.15	41.76	3.11	0.73	1.04	15.92
0-1*mm (3.2-6 mm)	1.04	43.69	23.45	31.82	41.12	3.06	0.72	0.96	15.63
0-1*mm (6-8 mm)	1.20	41.06	23.91	33.83	43.47	3.20	0.77	1.06	16.58
0-1*mm (8-10 mm)	1.18	39.74	24.45	34.63	44.99	3.29	0.79	1.00	17.20

(c) Honghe coal

Sample	Proximate analysis/%				Ultimate analysis/%				$Q_{net,ar}$/MJ·kg^{-1}
	M_{ar}	A_{ar}	V_{ar}	FC_{ar}	C_{ar}	H_{ar}	N_{ar}	S_{ar}	
0-1mm	2.74	26.82	37.57	32.87	47.84	3.56	1.42	3.57	18.15
1-2mm	2.80	22.03	38.85	36.32	51.49	3.76	1.52	3.33	19.55
2-3.2mm	3.06	19.78	39.57	37.59	53.34	3.91	1.54	3.38	20.30
3.2-6mm	2.86	20.59	39.59	36.96	53.30	3.97	1.56	3.28	20.29
0-1*mm (1-2 mm)	3.17	21.25	38.83	36.75	52.26	3.89	1.53	3.10	19.84
0-1*mm (2-3.2 mm)	3.10	19.99	39.28	37.63	53.16	3.98	1.56	3.17	20.19
0-1*mm (3.2-6 mm)	3.29	17.98	40.34	38.39	54.37	3.96	1.63	3.14	20.81

Data availability

Data will be made available on request.

References

[1] B. Leckner, Fluidized bed combustion: mixing and pollutant limitation, Prog. Energy Combust. Sci. 24 (1) (1998) 31–61, https://doi.org/10.1016/S0360-1285(97)00021-X.

[2] P. Basu, Combustion of coal in circulating fluidized-bed boilers: a review, Chem. Eng. Sci. 54 (22) (1999) 5547–5557, https://doi.org/10.1016/S0009-2509(99)00285-7.

[3] G.X. Yue, R.X. Cai, J.F. Lyu, H. Zhang, From a CFB reactor to a CFB boiler-the review of R&D progress of CFB coal combustion technology in China, Powder Technol. 316 (2017) 18–28, https://doi.org/10.1016/j.powtec.2016.10.062.

[4] A. Arjunwadkar, P. Basu, B. Acharya, A review of some operation and maintenance issues of CFBC boilers, Appl. Therm. Eng. 102 (2016) 672–694, https://doi.org/10.1016/j.applthermaleng.2016.04.008.

[5] J.F. Lyu, M.X. Shang, X.W. Ke, et al., Powdered coal circulating fluidized bed combustion technology, J. China Coal Soc. 48 (01) (2023) 430–437.

[6] M.X. Shang, Y.G. Yao, X.W. Ke, Z. Huang, T. Zhou, J.F. Lyu, Effect of back pressure on gas-solid dis-tribution characteristics of cyclone distributor applied in powdered coal-fired circulating fluidized bed combustion system, Powder Technol. 431 (2024) 119039, https://doi.org/10.1016/j.powtec.2023.119039.

[7] Q.Q. Ren, S.L. Bao, Combustion characteristics of ultrafine gasified semi-char in circulating fluidized bed, Can. J. Chem. Eng. 94 (2016) 1676–1682, https://doi.org/10.1002/cjce.22562.

[8] J.J. Li, M. Zhang, H.R. Yang, J.F. Lyu, X.X. Zhao, J.C. Zhang, The theory and practice of NOx emission control for circulating fluidized bed boilers based on the re-specification of the fluidization state, Fuel Process. Technol. 150 (2016) 88–93, https://doi.org/10.1016/j.fuproc.2016.05.004.

[9] F. Luis, C.A. Londono, X.S. Wang, B.M. Gibbs, Influence of operating parameters on NOx and N_2O axial profiles in a circulating fluidized bed combustor, Fuel 75 (8) (1996) 971–978, https://doi.org/10.1016/0016-2361(96)00045-2.

[10] X.W. Ke, M. Engblom, H.R. Yang, A. Brink, J.F. Lyu, M. Zhang, Prediction and minimization of NOx emission in a circulating fluidized bed combustor: a comprehensive mathematical model for CFB combustion, Fuel 309 (2022) 122133, https://doi.org/10.1016/j.fuel.2021.122133.

[11] B. Liang, H.L. Bai, B. Tan, L.L. Fu, D.R. Bai, Experimental investigation of circulating fluidized bed combustion of dry powders of coal slime, Fuel 348 (2023) 128566, https://doi.org/10.1016/j.fuel.2023.128566.

[12] G.X. Yue, L. Wang, Y. Li, Ash size formation characteristics in CFB coal combustion, in: Proceedings of 4th International Conference on Fluidized Bed Combustion. New York, 1993.

[13] S.X. Ma, J. Guo, W.M. Chang, G.X. Yue, H. Zhang, Study on the dynamic balance behaviors of b-ed material during the start-up process of a circulating fluidized bed boiler, Powder Technol. 280 (2015) 35–41, https://doi.org/10.1016/j.powtec.2015.04.043.

[14] H.B. He, N. Hu, J.F. Lyu, Q. Liu, J. Su, J.C. Zhang, X.X. Zhao, G.X. Yue, Analysis on additional sand size in low-ash fuel fired circulating fluidized bed boilers, J. Chin. Soc. Power Eng. 30 (2010) 409–414.

[15] M. Qian, A. Boelle, P. Jaud, Y.J. Na, Q.G. Lu, S.L. Bao, P. Cui, W.H. Jiao, H. M. Zhao, Influence of coal nature and structure on ash size formation characteristic and related pollutant emissions duri-ng CFB combustion, J. Therm. Sci. 9 (2000) 276–281.

[16] H.R. Yang, X.B. Xiao, J.F. Lyu, G.X. Yue, M. Qian, P. Jaud, Experimental technique on coal ash formation in CFB combustion, J. Chem. Ind. Eng. 54 (8) (2003) 1183–1187.

[17] J. Tomeczek, P. Mocek, Attrition of coal ash particles in a fluidized-bed reactor, AICHE J. 53 (2007) 1159–1163, https://doi.org/10.1002/aic.11140.

[18] Q. Zhang, T.J. Jamaleddine, C. Briens, F. Berruti, J. McMillan, Jet attrition in a fluidized bed. Part I: effect of nozzle operating conditions, Powder Technol. 229 (2012) 162–169, https://doi.org/10.1016/j.powtec.2012.06.025.

[19] J.G. Hao, Y.F. Zhao, M. Ye, Z.M. Liu, Influence of temperature on fluidized-bed catalyst attrition behavior, Chem. Eng. Technol. 39 (5) (2016) 927–934, https://doi.org/10.1002/ceat.201500660.

[20] O. Senneca, F. Scala, R. Chirone, P. Salatino, Relevance of structure, fragmentation and reactivity o-f coal to combustion and oxy-combustion, Fuel 201 (2017) 65–80, https://doi.org/10.1016/j.fuel.2016.11.034.

[21] Y.S. Chu, B. Davaabal, D.S. Kim, S.K. Seo, Y. Kim, C. Ruescher, J. Temuujin, Reactivity of fly a-shes milled in different milling devices, Rev. Adv. Mater. Sci. 58 (2019) 179–188, https://doi.org/10.1515/rams-2019-0028.

[22] D.F. Li, X.W. Ke, H.R. Yang, S.G. Ahn, J.F. Lyu, C.H. Jeon, M. Zhang, The ash formation and attrition characteristics of an Indonesia lignite coal ash for a 550 MWe ultra supercritical CFB boiler, Chem. Eng. Res. Des. 147 (2019) 579–586, https://doi.org/10.1016/j.cherd.2019.05.027.

[23] F. Winter, X. Liu, Attrition behavior of coal ash under circulating fluidized bed combustion conditions, in: Proceedings of the 17th International Conference on Fluidized Bed Combustion, American Society of Mechanical Engineering, New York, 2003, pp. 106–110.

[24] T. Wang, H.R. Yang, Y.X. Wu, Q. Liu, J.F. Lyu, H. Zhang, Experimental study on the effects of chemical and mineral components on the attrition characteristics of coal ashes for fluidized bed boilers, Energy Fuel 26 (2012) 990–994, https://doi.org/10.1016/j.cherd.2019.05.027.

[25] X. Yao, H. Zhang, H.R. Yang, Q. Liu, J.W. Wang, G.X. Yue, An experimental study on the prima-ry fragmentation and attrition of limestones in a fluidized bed, Fuel Process. Technol. 91 (2010) 1119–1124, https://doi.org/10.1016/j.fuproc.2010.03.025.

[26] H.R. Yang, G.X. Yue, X.B. Xiao, J.F. Lyu, Q. Liu, 1D modeling on the material balance in CFB boiler, Chem. Eng. Sci. 60 (2005) 5603–5611, https://doi.org/10.1016/j.ces.2005.04.081.

[27] Z. Tang, G.X. Yue, M. Qian, P. Jaud, The experimental investigation on the coal ash formation in CFB combustion, in: Proceeding of the 16th International Conference on Fluidized Bed Combustion, 2001.

[28] H.R. Yang, M. Wirsum, J.F. Lyu, X.B. Xiao, G.X. Yue, Semi-empirical technique for predicting as-h size distribution in CFB boilers, Fuel Process. Technol. 85 (2004) 1403–1414, https://doi.org/10.1016/j.fuproc.2003.09.003.
[29] D.F. Li, M.W. Kim, S.M. Kim, C.H. Jeon, K.J. Sung, H.R. Yang, X.W. Ke, R.X. Cai, M. Zhang, Mass balance study of a 550 MW supercritical CFB boiler with papsd method, in: Proceeding of the 23rd International Conference on Fluidized Bed Conversion, 2018.
[30] D. Merrick, J. Highley, Particle size reduction and elutriation in a fluidized bed process, AIChE Symp. Ser. 70 (137) (1974) 366–378.
[31] X.W. Ke, D.F. Li, M. Zhang, C.H. Jeon, R.X. Cai, J. Cai, J.F. Lyu, H.R. Yang, Ash formation characteristics of two Indonesian coals and the change of ash properties with particle size, Fuel Process. Technol. 186 (2019) 73–80, https://doi.org/10.1016/j.fuproc.2018.12.020.
[32] T.J. Jones, J.K. Russell, Ash production by attrition in volcanic conduits and plumes, Sci. Rep. 7 (2017) 5538, https://doi.org/10.1038/s41598-017-05450-6.